JOURNAL OF CELLULAR PHYSIOLOGY 209:56–66 (2006)

Regulation of Angiogenesis and Tumor Growth by p110 Alpha and AKT1 via VEGF Expression

CHANG XIA,[1] QIAO MENG,[1] ZONGXIAN CAO,[1] XIANGLIN SHI,[2] AND BING-HUA JIANG[1]*

[1]*Mary Babb Randolph Cancer Center, Department of Microbiology, Immunology and Cell Biology, West Virginia University, Morgantown, West Virginia*

[2]*Health Effects Laboratory Division, National Institute for Occupational Safety and Health, Morgantown, West Virginia*

Recent studies demonstrate that PI3K activation and PTEN mutation are frequently found in many human cancer cells and tissues. However, the mechanism of PI3K signaling in human cancer tumorigenesis remains to be elucidated. In this study we specifically downregulated p110α expression in ovarian cancer cells using siRNA interference. We found that p110α downregulation greatly decreased ovarian tumor growth and angiogenesis, and that p110α siRNA inhibited VEGF expression through decreasing hypoxia-inducible factor 1α expression in both ovarian cancer cells and tumor tissues. To determine the downstream targets of PI3K in regulating tumor growth and angiogenesis, we find that AKT1 is a major downstream mediator for regulating tumor growth, angiogenesis, and VEGF expression. These data show that p110α and AKT1 play an important role in tumor growth by inducing angiogenesis and by increasing HIF-1α and VEGF expression. This work provides a better understanding of the molecular mechanism of human cancer induced by the activation of PI3K signaling. J. Cell. Physiol. 209: 56–66, 2006. © 2006 Wiley-Liss, Inc.

Ovarian cancer is the most common cause of death from gynecological disease for women in Western countries (Bertone-Johnson, 2005). Most often, late diagnosis of the disease makes it impossible to remove all ovarian lesions by surgery. The difficulty of detecting the disease in its early stages and the propensity of ovarian cancer cells to develop resistance to known chemotherapeutic treatments dramatically decreases the 5-year survival rate of ovarian cancer patients (Vergote and Trimbos, 2003; Trimbos and Timmers, 2004). Different subunits of phosphatidylinositol 3-kinase (PI3K) have been implicated in a number of human cancers, such as ovarian, breast, gastric, and hepatocellular carcinoma (Lee et al., 2004; Sansal and Sellers, 2004). PI3K has been shown to play a role in cell proliferation and anti-apoptosis, which are crucial to cancer development (Andrew, 1999). The increased copy number of the p110α catalytic subunit of PI3K was observed in approximately 40% of ovarian cancer occurrences (Shayesteh et al., 1999). The somatic mutations of PIK3CA gene, which encodes p110α catalytic subunit, were also found with significant high frequency in colorectal, cervical, ovarian, and breast cancers (Ma et al., 2000; Broderick et al., 2004; Samuels and Velculescu, 2004; Samuels et al., 2004; Tong et al., 2004). Besides p110α mutation, somatic mutations of p85 were found in primary human colon and ovarian cancer cells (Philp et al., 2001; Jucker et al., 2002; Hallmann et al., 2003). Furthermore, the tumor suppressor PTEN, an antagonist of PI3K, is frequently lost in ovarian cancer. The reduction of PTEN expression is correlated with the progression of ovarian cancer (Obata et al., 1998; Yokomizo et al., 1998; Schondorf et al., 2000; Idoate et al., 2003). These data indicate that PI3K activation plays an important role in ovarian cancer progression. In this study, we will focus on the mechanism of PI3K in regulating ovarian tumor growth.

PI3K is composed of p85 regulatory and p110α catalytic subunits. PI3K is activated upon the recruitment of the inactive p85 subunit to the membrane in response to an appropriate physiologic stimulation (Carpenter and Cantley, 1990; Carpenter et al., 1990; Carpenter et al., 1993; Rameh et al., 1995; Carpenter and Cantley, 1996). At the membrane, PI3K phosphorylates phosphatidylinositol-4,5-bisphosphate (PIP2) at the 3′ position on its inositol ring and converts PIP2 to PIP3. Subsequently, PIP3 recruits other downstream molecules via binding to their pleckstrin-homology (PH) domains (Klippel et al., 1996). AKT, a serine/threonine protein kinase, is one of the most important downstream targets of PI3K. AKT transmits oncogenic signals and mediates a variety of cellular responses including cell growth, transformation, differentiation, motility, and cell survival. Because AKT and its upstream regulators are deregulated in a wide range of solid tumors and hematologic malignancies, AKT has been implicated in playing a pivotal role in malignant transformation and chemoresistance by inducing cell survival, growth and migration (Bos, 1995; Datta et al., 1996; Franke et al., 1997; Hemmings, 1997).

Recent studies show that PI3K inhibitor LY294002 decreased cell proliferation, and induced cell cycle arrest in ovarian cancer cells. Wortmannin treatment induced cell differentiation, and inhibited colon tumor growth in vivo (Stein, 2001; Bedogni et al., 2004; Marley et al.,

Abbreviations: PI3K, phosphatidylinositol 3-kinase; PIP2, phosphorylates phosphatidylinositol-4,5-bisphosphate; PIP3, phosphatidylinositol 3,4,5-trisphosphate; siRNA, small interfering RNA; VEGF, vascular endothelial growth factor; HIF-1α, hypoxia-inducible factor-1alpha.

Contract grant sponsor: American Cancer Society Research Scholar; Contract grant number: 04-076-01-TBE; Contract grant sponsor: National Cancer Institute; Contract grant number: CA109460.

*Correspondence to: Bing-Hua Jiang, Mary Babb Randolph Cancer Center, Department of Microbiology, Immunology and Cell Biology, West Virginia University, Morgantown, WV 26506-9300. E-mail: bhjiang@hsc.wvu.edu

Received 23 February 2006; Accepted 8 May 2006

DOI: 10.1002/jcp.20707

2004). However, LY294002 and Wortmannin can inhibit different isoforms of PI3K as well as other kinases. Therefore, in this study we used siRNA to target p110α subunit. SiRNA inhibits gene expression through the post-transcriptional gene-silencing (PTGS) mechanism by inducing the degradation of the target gene mRNA. SiRNA can silence a specific gene to study its physiological effects. Here, we aim to explore the function of PI3K/AKT signaling in tumor growth and angiogenesis by specifically silencing p110α and AKT1, which would be important to study the mechanism of ovarian tumorigenesis.

Angiogenesis is the formation of new blood vessels from the pre-existing vasculature. Angiogenesis is required for tumor growth beyond 1–2 cm in size (Folkman, 1971; Folkman, 1974). Angiogenesis creates a strong vascular network that enhances tumor growth and the potential of metastasis. Vascular endothelial growth factor (VEGF) is a secreted glycoprotein specific to endothelial cells and is a potent angiogenesis inducer. VEGF binds to its receptor VEGFR-1, VEGFR-2, and VEGFR-3 to regulate neovascularization in the tumor (Neufeld et al., 1999; McMahon, 2000). It is known that many tumor cells produce high levels of VEGF. The increase of serum VEGF levels in tumors is associated with poor clinical outcome (Brown et al., 1999; McMahon, 2000). VEGF expression is regulated at transcriptional level by hypoxia-inducible factor 1 (HIF-1) in response to hypoxia and growth factor stimulation. HIF-1 is a heterodimer of HIF-1α and HIF-1β subunits (Wang and Semenza, 1993; Semenza et al., 1994; Jiang et al., 1996). HIF-1α expression can be induced by hypoxia, growth factors, and oncogenes. Activation of PI3K has been shown to increase levels of HIF-1α, and these levels correlated with tumorigenicity and angiogenesis in nude mice (Mazure et al., 1997; Zhong et al., 2000; Zundel et al., 2000; Laughner et al., 2001; Trisciuoglio et al., 2005).

The PI3K/AKT signaling pathway is involved in growth factor signaling cascades. P85 has been shown to be constitutively associated with the VEGF receptor Flk-1/KDR. The activation of Flk-1/KDR by VEGF promoted the tyrosine autophosphorylation of Flk-1/KDR, and also induced phosphorylation of p85. This led to an increase in PI3K and MAP kinase activities to mediate endothelial cell proliferation (Suzuma et al., 2000; Dayanir et al., 2001). VEGF-induced endothelial cell survival in vitro was blocked by PI3K inhibitors Wortmannin and LY294002 (Qi et al., 1999; Thakker et al., 1999). The activation of PI3K pathway is associated specifically with late-stage and high-grade ovarian tumors, due to the observation that both PI3K and VEGF are overexpressed in ovarian carcinoma, where VEGF exerts important biological functions such as promoting both tumor growth and the formation of ovarian cysts and ascites (Campbell et al., 2004; Chakravarti et al., 2004). We have recently shown that overexpression of v-P3k, a homolog of the PI3K catalytic subunit p110α, can induce angiogenesis in chicken embryos, and that PI3K activation correlates with an increase of VEGF levels in the CAM model in vivo, suggesting an important role of PI3K in angiogenesis (Jiang et al., 2000). We also showed that AKT expression induces angiogenesis (Jiang et al., 2001). Although the existing literature strongly suggests a linear connection between PI3K/Akt and VEGF regulation, some study showed that HIF-1 is dispensable for Akt oncogenic and angiogenic effects and that HIF-1 and Akt independently promote tumor growth and angiogenesis in vivo (Arbiser et al., 1997b; Arsham et al., 2002). The specific roles of PI3K and AKT in tumor-induced angiogenesis in vivo remain to be elucidated via approaches of better specificity.

MATERIALS AND METHODS

Reagents and cell culture

The human ovarian cancer cells OVCAR-3 were maintained in RPMI 1640 medium (Invitrogen, Carlsbad, CA) supplemented with 10% fetal bovine serum (FBS), 2 mM L-glutamine, 100 units/ml penicillin, and 100 μg/ml streptomycin; and cultured at 37°C in a 5% CO_2 incubator. Trypsin (0.25%)/EDTA solution was used to detach the cells from the culture flask for passing the cells. Antibodies against phospho-AKT (Ser473), AKT, AKT (5G3) Mouse mAb, phospho-ERK were from Cell Signaling Technology (Beverly, MA). Antibodies against HIF-1 and HIF-1β were from BD Biosciences (Bedford, MA). Antibody against VEGF was purchased from R&D (Minneapolis, MN). PI3K inhibitor LY294002 was from Calbiochem (La Jolla, CA).

Generation of siRNA constructs

To achieve siRNA-induced p110α and AKT1 silencing, a homology analysis with the National Center for Biotechnology Information's Basic Local Alignment Search Tool (BLAST) was used to design a siRNA, and two targets were selected, which would target the 19-bp RNA sequence of PI3K p110α and AKT1 mRNA, respectively. The sense sequence is as follows: siP1: TGATGCACATCATGGTGGC; siP2: AGTTCCCAGAT ATGTCAGT; siA1: GAAGGAAGTCATCGTGGCC; siA2: GATGACAGCATGGAGTGTG. To generate hairpin siRNA, two annealed 69-mer sense and antisense DNA oligonucleotides containing the 19-mer sequence directed against PI3K p110α and AKT1 mRNA, respectively, were ligated into pSilencer^{TM} 2.1-U6 neo vector (Ambion Inc. Austin, TX), named as pSilencer-siP1, pSilencer-siP2, pSilencer-siA1, and pSilencer-siA2, respectively. In addition, 69-mer DNA oligonucleotides containing the 19-mer scramble sequence having no homology to any human genomes were also ligated into the vector, and used as the control, named as pSilencer-siSCR. The final expression construct contained a U6 promoter that directs the synthesis of oligonucleotides in an inverted repeat with 9 bp for its loop and 6 Ts added at the end to serve as a termination signal for RNA polymerase III. After the transcription, the RNA is expected to fold back to form a hairpin loop structure (Fig. 1A).

Establishment of stable cell lines expressing siRNA constructs

To establish stable cell lines expressing the siRNA constructs, OVCAR-3 cells were transfected with the pSilencer carrying siRNA against PI3K p110α, AKT1 mRNA or scramble sequence containing the same length of sequence without homolog to any known human gene. Lipofectamine was used by the standard procedure according to the manufacturer's instructions (Invitrogen). Following the transfection, the cells were cultured for 24 h, followed by the addition of 500 μg/ml G418 and culture for 2 weeks to obtain stable cell lines. Multiple geneticin-resistant colonies were then pooled after 2 weeks of selection. In abbreviation, siSCR is scramble siRNA, siP1 and siP2 are two siRNA constructs against PI3K p110α, and siA1 and siA2 are two siRNA constructs against AKT1.

Northern blot analysis

Cells cultured to 90% confluence were harvested, and total cellular RNAs were isolated using the Trizol reagent (Life Technologies, Carlsbad, CA). Aliquots (15 μg) of total cellular RNAs were fractionated through 1% agarose containing 2.2 M formaldehyde and transferred to Hybond^{+} nylon membranes (Amersham, Piscataway, NJ). The AKT1 cDNA probes were labeled by ^{32}p using the random primer method. The RNAs in the membranes were detected by the cDNA probes in QuickHyb solution (Stratagene, La Jolla, CA) following the manufacturer's instruction. To monitor RNA loading and

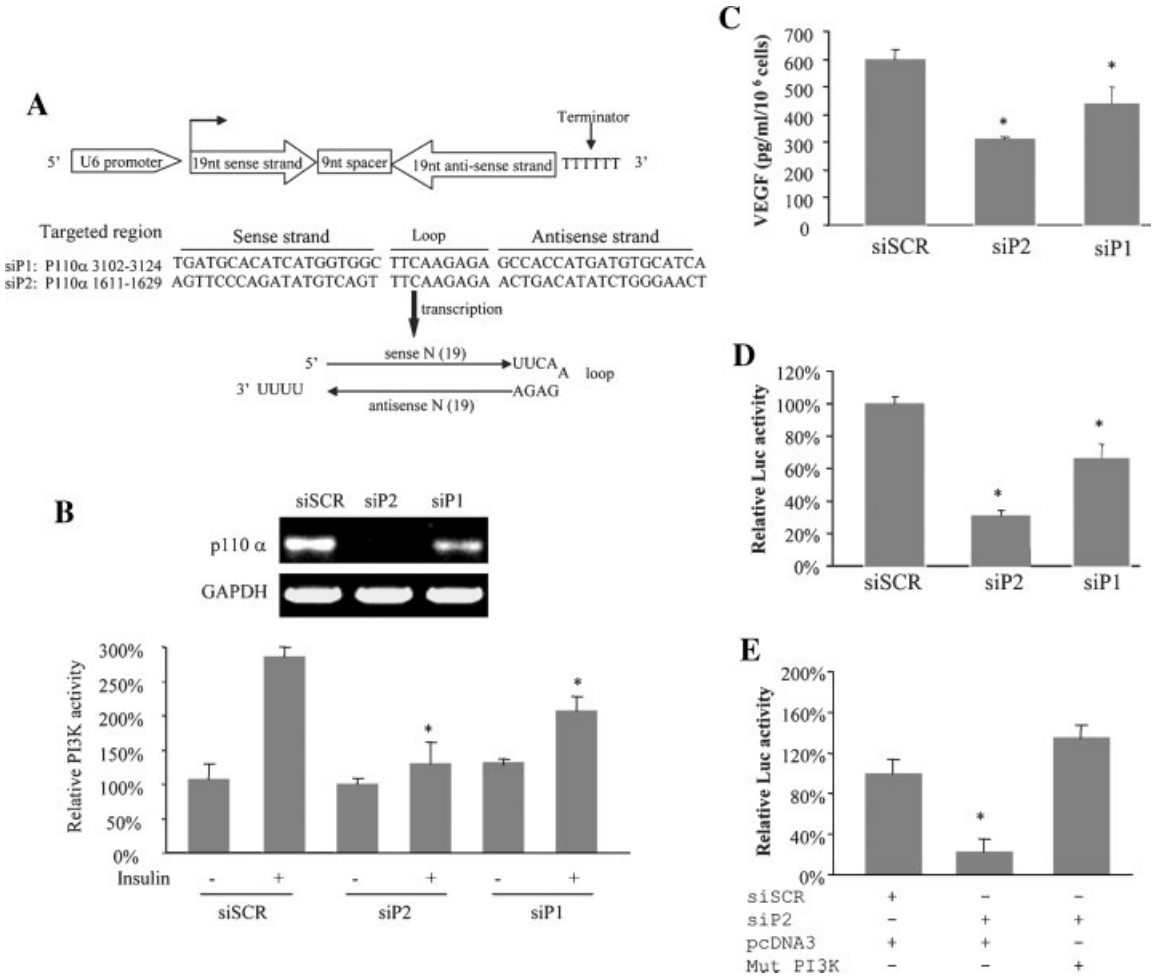

Fig. 1. SiRNA against p110α inhibits p110α expression and PI3K activation. **A**: Schematic representation of the siRNA construct in pSilencer^{TM} 2.1-U6 neo vector, in which p110α siRNA construct was based on the specific 19 bp sense sequences of p110α mRNA. **B**: OVCAR-3 cells were transfected with the pSilencer carrying siRNA against p110α subunit (siP1 and siP2) or the vector (siSCR) containing the same length of sequence without homolog to any known human gene. Cells were selected by 500 μg/ml G418 to obtain stable cell lines. Upper part: The effects of siP1 and siP2 on p110α mRNA levels were analyzed by RT-PCR. GAPDH mRNA levels were used as an internal control. Lower part: PI3K kinase activity in OVCAR-3 cells expressing siP1, siP2, or the scramble siRNA. The cells were cultured to 80% confluence, followed by serum starvation for 24 h, then stimulated with 100 nM insulin for 1 h. Aliquots of total proteins (300 μg) were diluted with lysis buffer to the final volume of 400 μl for PI3K activity assay with phosphatidylinositol as substrate, analyzed by the incorporation of ^{32}P into the lipid product, and detected by autoradiography. PI3K kinase signals were quantified by densitometry from three independent experiments, and normalized to those of the untreated serum-starved cells. **C**: OVCAR-3 cells were seeded in 12-well plates the day before transfection. The old medium was discarded and fresh medium was supplemented when the cells reached 90% confluence. The supernatant was collected 24 h after the incubation. VEGF protein levels in the supernatant were determined by ELISA, and divided by the number of cells in each dish. The data are presented as the mean ± SD from three independent experiments with triplicate cultures per experiment. **D**: The cells were seeded at 0.5×10^6 cells/well in 12-well plates, and cultured overnight. The cells were co-transfected with pCMV-β-gal (0.2 μg), pVEGF-Luc plasmids (1 μg), and 1 μg of pSilencer carrying the scramble siRNA, siP2 or siP1. The cells were cultured for 48 h after transfection. The relative luciferase activity was calculated by the ratio of luc activity/β-gal, and normalized to that of the control. **E**: OVCAR-3 were co-transfected with pCMV-β-gal (0.2 μg), pVEGF-Luc plasmids (1 μg), and 1 μg of pSilencer carrying the scramble siRNA, siP2 with the vector or mutant PI3K with 3-bp mutation in the target sequence. The cells were cultured for 48 h after transfection. The relative luciferase activity was calculated by the ratio of luc activity/β-gal, and normalized to that of the control. * indicates that the value was significantly different when compared to that of the scramble siRNA control ($P < 0.01$).

transferring efficiency, different regions of the membranes were hybridized with a β-actin cDNA probe.

Semi-quantitative RT-PCR

Total RNAs were isolated with Trizol reagent (Life Technologies). First-strand cDNA was synthesized from 1 μg of total RNA using AMV Reverse Transcriptase, an oligo(dT) primer and dNTP (Promega, Madison, WI). Primers used for amplification were as follows: PI3K p110α sense: 5′-TATGGTTGTCTGTCAATCGGTGA-3′; PI3K p110α antisense: 5′-GCCTTTGCAGTGAATTTGCAT-3′; GAPDH sense: 5′-CCACCCATGG CAAATTCCATGGCA-3′; GAPDH antisense: 5′-TCTAGACGGCAGGTCAGGTCCACC-3′. The PCR products for p110α and GAPDH are 145 and 550 bp, respectively. Each RT-PCR reaction consisted of 30 cycles of 1 min at 94°C, 1 min at 55°C and 1 min at 72°C. Quantification of the amount of PCR product after 30 cycles was performed after electrophoresis on 2% agarose gels and ethidium bromide staining.

PI3K assay

Cells were washed with ice-cold PBS, scraped from the plates, and centrifuged at 4,000 rpm for 5 min. The cell pellets were incubated for 20 min on ice in lysis buffer (150 mM NaCl, 100 mM Tris-HCl (pH 8.0), 1% Triton X-100, 5 mM EDTA, 10 mM NaF) supplemented with 1 mM dithiothreitol, 1 mM phenylmethylsulfonyl fluoride, 1 mM sodium vanadate, 2 mM leupeptin, and 2 mM aprotinin, and centrifuged at 15,000*g* for 15 min to clarify the supernatants. PI3K activity was analyzed

using 300 μg of protein extracts and anti-p110α antibodies as we described previously. Briefly, 300 μg of total proteins were adjusted to 400 μl with the lysis buffer, and were then incubated with 10 μl of antibodies against PI3K catalytic subunit p110α for 2 h at 4°C. Protein A/G-agarose beads (15 μl) were added and incubated for 1 h. The beads were then pelleted and washed sequentially with TNE buffer (containing 20 mM Tris, pH 7.5, 100 mM NaCl, and 1 mM EDTA) three times, and once with 20 mM HEPES. PI3K activities were assayed using phosphatidylinositol as substrate in a final volume of 50 μl containing 20 mM HEPES (pH 7.5), 10 mM MgCl, 2 μCi of [γ-^{32}P] ATP, 60 μM ATP, and 0.2 mg/ml sonicated phosphatidylinositol. Reactions were carried out for 15 min at room temperature, and the reaction tubes were agitated every 3 min. The reaction was terminated by adding 80 μl of 1 M HCl, and end products were extracted by the addition of 160 μl of chloroform/methanol (1:1). After centrifugation, the organic phase was evaporated to dryness and separated on a TLC plate. PI3K activity was analyzed by the incorporation of ^{32}P into phosphorylated lipids and detected by autoradiography.

Densitometry analysis

Autoradiographic signals of immunoblotting and PI3K activity assays were quantified using molecular analyst/PC densitometry software (Bio-Rad, Hercules, CA). Mean densitometry data from independent experiments were normalized to that obtained from the cells in the control. The data were presented as the mean ± SD and analyzed by the unpaired Student's *t* test.

Immunoblotting analysis

The cells were plated in a 60-mm culture dish and lysed in RIPA buffer (150 mM NaCl, 100 mM Tris (pH 8.0), 1% Triton X-100, 1% deoxycholic acid, 0.1% SDS, 5 mM EDTA, and 10 mM NaF) supplemented with 1 mM sodium vanadate, 2 mM leupeptin, 2 mM aprotinin, 1 mM phenylmethylsulfonyl fluoride, 1 mM dithiothreitol, and 2 mM pepstatin A on ice for 30 min. After centrifugation at 14,000 rpm for 15 min, the supernatant was harvested as the total cellular protein extracts and stored at −70°C. The protein concentrations were determined using Bio-Rad protein assay reagents. The total cellular protein extracts were separated by 7% SDS–PAGE, and transferred to nitrocellulose membrane in 20 mM Tris-HCl (pH 8.0) containing 150 mM glycine and 20% (v/v) methanol. Membranes were blocked with 5% nonfat dry milk in 1× TBS containing 0.05% Tween 20 and incubated with antibodies against phospho-AKT (Ser473), AKT, HIF-1 and HIF-1β. Protein bands were detected by incubation with horseradish peroxidase-conjugated antibodies (Perkin-Elmer Life Sciences, Wellesley, MA), and visualized with enhanced chemiluminescence reagent (Perkin-Elmer Life Sciences).

Enzyme-linked immunosorbent assay

Capture enzyme-linked immunosorbent assay was performed using human VEGF antibody (BAF493, R&D Systems) as capture antibody and anti-VEGF164 biotinylated antibody (AF-493-NA, R&D Systems) as detection antibody in the concentrations per the manufacturer's instruction. The reaction plate was revealed by the 2,2′-aziro-bis-(3-ethylbenzothiazoline-g-sulfonic acid) diammonium salt (ABTS) detection system (Roche, Indianapolis, IN) after the incubation with streptavidin-horseradish peroxidase (Pharmingen, San Diego, CA). Optical densities were read at 405 nm and VEGF concentrations were determined by the comparison to standard curves generated with recombinant human VEGF164 (R&D Systems). The rate of VEGF secretion was calculated as we previously described (Fang et al., 2004; Skinner et al., 2004b).

Luciferase assay

To assay the transcriptional activation of VEGF, OVCAR-3 cells in 12-well plates were transiently co-transfected with the human VEGF reporter plasmid (1 μg) and β-galactosidase (0.2 μg) as a control for transfection efficiency. The cells were cultured for 48 h after the transfection, and luciferase activities were analyzed as we described (Skinner et al., 2004a). Briefly, the luciferase activity was measured using a chemiluminometer Wallac 1420, and β-gal activity was assayed by the incubation of cell lysates with a 2× β-galactosidase assay buffer (200 mM sodium phosphate buffer, pH 7.8, 2 mM $MgCl_2$, 100 mM β-mercaptoethanol, 1.33 mg/ml ?-nitrophenyl β-D-galactopyranoside). The absorbance at 420 nm was measured with a spectrophotometer Wallac 1420. The relative Luc activity was calculated by the ratio of luc/β-gal activity, and normalized to that of the control.

Tumor-induced angiogenesis on chicken chorioallantoic membrane (CAM)

White Leghorn chicken eggs were fertilized and incubated at 37°C under conditions of constant humidity. The developing CAM was separated from the shell by opening a window at the broad end of the egg above the air sac at Day 9. The opening was sealed with Parafilm (American National Can, Chicago, IL) and the eggs were returned to the incubator. To investigate the effect of LY29004 on tumor-induced angiogenesis, human ovarian cancer OVCAR-3 cells were trypsinized, washed, and resuspended at 2×10^7 cells/ml in serum-free RPMI 1640, which contained 5% Matrigel (Collaborative Biomedical Products, Bedford, MA) in the absence or presence of LY29004. Aliquots of the mixture were then applied to the CAM of 9-day-old embryos. After 96 h incubation, the area around the implanted Matrigel was photographed with a Nikon digital camera, and the numbers of newly formed vessels were counted by two observers in a double-blind manner. Assays for each treatment were carried out using 8–10 embryos per experiment.

Tumor sections and immunostaining

The tumors were cut into half, and fixed in 10% formaldehyde overnight, then embedded in paraffin (OCT; Miles, Indiana). The sections at 5 μm were prepared from peripheral region of the tumor to avoid central necrosis, and collected on positively charged slides (Wax-It Histology Services, B.C., Canada). Sections were deparaffinized in xyline for 5 min, in absolute alcohol for 5 min, in 95% alcohol for 3 min, and in 70% alcohol for 3 min, then rinsed three times in deionized water. The slides were then steamed with antigen retrieval buffer (10 mM citrate, pH 8.0) for 10 min, cooled to room temperature for 20 min, then rinsed three times in deionized water. The slides were incubated with 5% goat serum at room temperature for 1 h, then stained with antibodies against VEGF, HIF-1α, PCNA or p-AKT (Ser473) overnight at 4°C, followed by the incubation with a FITC conjugated anti-rabbit or anti-mouse secondary antibodies (Jackson Laboratories, Bar Harbor, Maine) for 1 h at room temperature. The sections were washed three times with PBS buffer between each step. The stainings were examined with a Zeiss Axiovert 100 TV microscope with a 40 × 1.4 objective lens equipped with a laser scanning confocal attachment (LSM 510; Zeiss). Quantification of immunofluorescence intensity was performed with the NIH Image software (Bethesda, MD). To quantify the fluorescein positive pixels, the channels were split into red, green, and blue, with all further analysis done on the green channel. Background fluorescence was subtracted, and the image was binarized to the black and white. The fraction of white pixels was quantified. The final specific values for the pixel intensity of immunostaining on the tumor sections was derived from the result of the raw pixel intensity values subtracted by the pixel intensity values of the surrounding tissue. At least two tumors were used for the preparation of tissue sections, three different sections were randomly chosen for the imaging and quantification.

TUNEL assays

Transferase-mediated dUTP nick end labeling (TUNEL) staining was used to examine apoptosis. Negative controls were stained in the absence of terminal deoxynucleotidyl transferase enzyme. Tissues harvested from the CAM were fixed in 10% formaldehyde overnight and paraffin-embedded. Sections at 5 μm in thickness were deparaffinized, rehydrated, and permeabilized using 0.1% Triton X-100 in 0.1% sodium

citrate to perform TUNEL assays as described by the manufacturer (Roche Diagnostics).

Statistical analysis

The data were analyzed using SPSS statistics software package (SPSS, Chicago, IL). All of the results are expressed as mean ± SD, and the difference was considered significant at $P < 0.05$ or $P < 0.01$.

RESULTS

SiRNA against PI3K catalytic subunit p110α inhibited p110α expression and PI3K activity in ovarian cancer cells

Our previous study showed that inhibition of PI3K activity using PI3K inhibitor LY294002 decreased cell proliferation and G_1 progression in ovarian cancer cells (Gao et al., 2004). However, LY294002 can inhibit different isoforms of PI3K, and affect both the cancer cells and host cells in vivo. Therefore, in this study we investigated the role of p110α catalytic subunit in ovarian tumor growth and angiogenesis by specifically inhibiting its expression using siRNA against p110α subunit. In order to achieve this goal, we constructed two vectors expressing siRNA against p110α, called siP1 and siP2, respectively; and established stable cell lines. The effect of siRNA expression on p110α mRNA levels was analyzed by RT-PCR. Compared to scramble siRNA control, siP1 and siP2 expression in the cells significantly reduced the levels of p110α mRNA (Fig. 1B). GAPDH levels were used as an internal control. To test whether siP1 and siP2 decreased PI3K kinase activity, serum-starved OVCAR-3 cells expressing siP1, siP2 or the scramble siRNA were stimulated with 100 nM insulin. Insulin treatment greatly induced PI3K activity in the OVCAR-3 cells expressing scramble siRNA, while the cells expressing siP1 and siP2 had significantly lower PI3K activity (Fig. 1B). We also found that siP1 and siP2 inhibited VEGF protein levels when compared to the siSCR-expressing cells (Fig. 1C), indicating that inhibition of p110α subunit was sufficient to decrease VEGF production in the cells. To further determine the mechanism through which PI3K regulates VEGF expression, the cells were transiently transfected with a VEGF luciferase reporter containing 2.6-kb human VEGF promoter (Forsythe et al., 1996c). VEGF reporter activity was significantly decreased in siP1- and siP2-expressing cells when compared to the control cells (Fig. 1D). These results showed that p110α subunit regulates VEGF expression at the transcriptional level. This result showed that p110α subunit was required for insulin-induced PI3K activity in the cells, suggesting that PI3K siRNA expression is sufficient to decrease PI3K activation.

In order to test the specificity of siP2 to knockdown p110α subunit, cells were co-transfected with VEGF luciferase reporter and pSilencer plasmid carrying siP2 or the scramble siRNA with a mutant p110α subunit with 3-bp mutation in the siRNA targeting sequence. The mutation of p110α subunit completely abolished the knock-down effect of siP2 in inhibiting VEGF transcriptional activation (Fig. 1E).

SiP2 inhibited cancer cell-induced angiogenesis and tumor growth in vivo

To address whether PI3K inhibitor LY294002 could inhibit ovarian tumor-induced angiogenesis, we used the CAM assay to study angiogenesis. The Matrigel was mixed with the cancer cells in the presence or absence of LY294002. Quantitative analysis showed that OVCAR-3 cells induced a fourfold higher rate of angiogenesis than the basal level in the CAM with Matrigel alone (Fig. 2A). The tumor-induced angiogenesis was inhibited by LY294002 treatment by more than 50% inhibition (Fig. 2A). These data demonstrated that LY294002 decreased ovarian cancer cell-induced angiogenesis.

To test whether specific inhibition of p110α subunit affected tumor-induced angiogenesis in vivo, OVCAR-3 cells expressing siP2 or scramble siRNA were mixed with Matrigel, and implanted onto the CAM of 9-day-old embryos, and incubated for 4 days at 37°C. Compared to the control, siP2 expression completely decreased ovarian tumor-induced angiogenesis to the basal level of the Matrigel alone without any visible effects on the pre-existing blood vessels (Fig. 2B,C). The tumor weight is similar in the same experiment (Fig. 2C). This result showed that p110α subunit expression is important for ovarian cancer cells to induce angiogenesis. To test the effect of siP2 on tumor growth, the cells were mixed with Matrigel, and implanted onto the CAM to grow tumors for 9 days as described above. SiP2 expression greatly inhibited tumor growth. Tumor volume with siP2 expression was only 25% of that in the control (Fig. 2D). This result suggests that siP2 initially inhibited angiogenesis, then inhibited tumor growth. To study whether siP2 inhibited cell proliferation in the tumors, the tissue sections were stained with antibodies against PCNA, a cell proliferation marker. A high amount of PCNA staining was observed in the control tumors while siP2 greatly decreased the PCNA expression (Fig. 2E). These results suggest that siP2 inhibits cell proliferation in the tumors. To evaluate the effect on apoptosis, TUNEL assay was performed on tumor sections. There was much more apoptosis in the tissues with the expression of siP2 than in those expressing siSCR (Fig. 2F).

SiP2 inhibited VEGF expression through HIF-1α expression

To test whether siP2 inhibits VEGF transcriptional activation through HIF-1 DNA binding, we employed a short form of VEGF luciferase reporter, pMAP11wt, consisting of the HIF-1 binding site and the adjacent functional promoter region (Forsythe et al., 1996b; Fang et al., 2005). The cells were co-transfected with pMAP11wt reporter and siP2 constructs. The cells treated by LY294002 were used as a control. SiP2 expression greatly decreased pMAP11wt reporter activity (Fig. 3A). This result is consistent with the effects of LY294002, which decreased VEGF transcriptional activity in a dose-dependent manner (Fig. 3A). In order to confirm the specificity of reporter assay, the cells were also co-transfected with pMAP11mut reporter, which was mutated with 3-bp substitution at the HIF-1 DNA binding site. We found that siP2 and LY294002 no longer inhibited the mutant reporter activity, suggesting that p110α subunit regulates VEGF transcriptional activation through the HIF-1 DNA binding site (Fig. 3A). To determine the effect of siP2 on HIF-1 protein expression, the cells were cultured in serum-free medium overnight and treated with insulin for 6 h. Whole cellular lysates were analyzed by immunoblotting using antibodies against HIF-1α and HIF-1β proteins. Insulin specifically induced HIF-1α, but not HIF-1β expression in the cells. SiP2 abolished HIF-1α expression, suggesting that PI3K may activate VEGF transcription through HIF-1α expression in the cells (Fig. 3B).

To test whether p110α subunit plays an important role in VEGF and HIF-1α expression in tumors, tumor

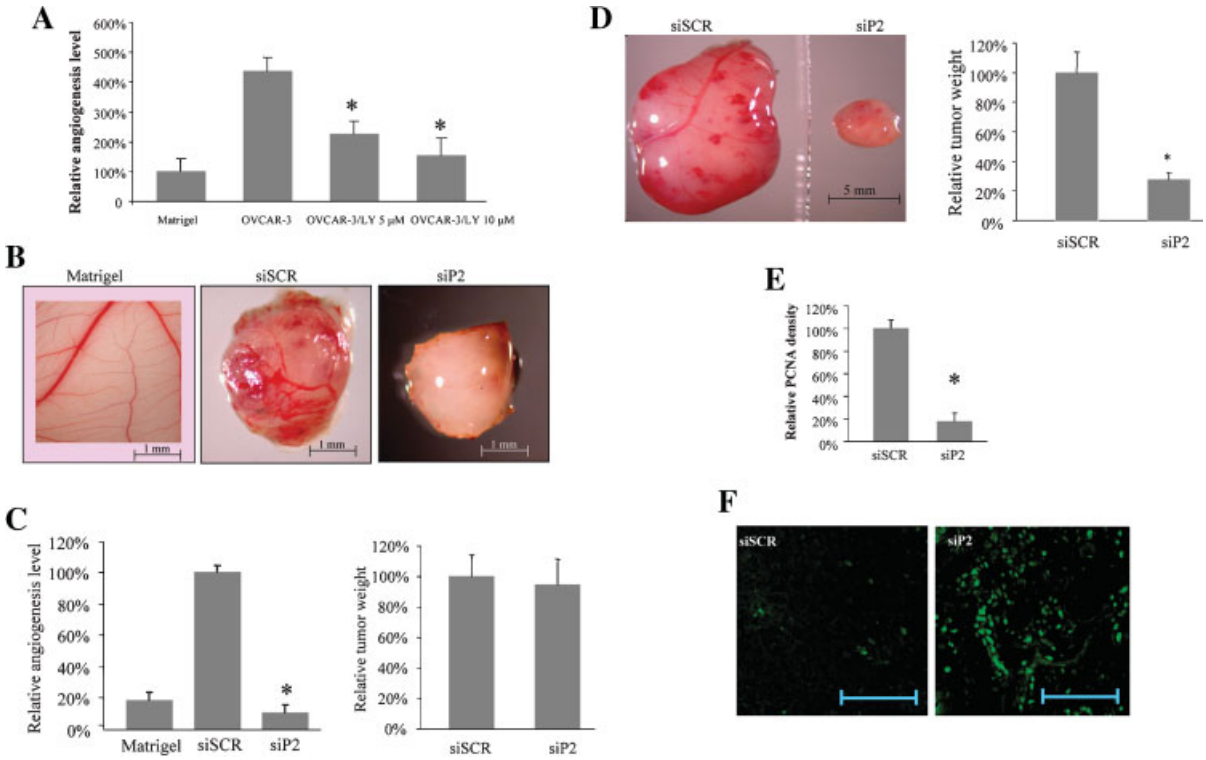

Fig. 2. Inhibition of PI3K activity decreased ovarian cancer cell-induced angiogenesis and tumor growth in vivo. **A**: 3×10^6 ovarian cancer cells were mixed with Matrigel in the absence or presence of 5 μM LY294002, and implanted onto the CAMs of 9-day-old chicken embryos. The Matrigel mixed with medium alone was used as a negative control. After implantation for 96 h, blood vessels were counted on the CAM by counting the branching of blood vessels. The number of blood vessels was obtained from the CAMs of 8–10 embryos per treatment. The data represent the mean ± SD of blood vessel number from replicate experiments, and were normalized to the Matrigel alone control. **B**: Matrigel was mixed with OVCAR-3 cells expressing the siP2 or scramble siRNA, and were implanted onto the CAM as described above. Matrigel alone was used as a negative control. The photos are representative tumors on the CAM. **C**: Left part: The relative angiogenesis was analyzed on the CAM 96 h after the implantation, and normalized to that expressing the scramble siRNA. Right part: the relative tumor weight in the same experiments. The data represent the mean ± SD from 10 replicate embryos. * indicates significantly different when compared to the scramble siRNA control ($P < 0.01$). **D**: Representative tumors of each treatment. Equal number of the cells (3×10^6 cells) were mixed with Matrigel and implanted onto the CAMs of 9-day-old chicken embryos. Tumor growth was monitored 9 days after the implantation. Left part: the representative tumors. Right part: relative tumor weight was obtained from the CAMs of 8–10 embryos per treatment. The data represent the mean ± SD of the relative tumor weight which is normalized to the control. **E**: The tumor tissue sections were stained with antibodies against PCNA. Images were captured and analyzed by confocal fluorescence microscope. Relative density of immunofluorescent staining was quantified as described in Materials and Methods. * indicates that the value was significantly different when compared to that of the siSCR control ($P < 0.01$). **F**: TUNEL staining. Positively stained fluorescein-labeled tumor sections were visualized and photographed by fluorescence microscopy. The scale bar represents 100 μm.

sections were analyzed by immunohistochemistry using antibodies against VEGF and HIF-1α. The knockdown of p110α subunit by siP2 significantly decreased VEGF and HIF-1α expression in the tumors (Fig. 3C,D). Similar result was obtained when HIF-1α expression from tumor tissues was analyzed by immunoblotting (Fig. 3D). HIF-1β and β-actin levels were not affected. These data demonstrate that p110α subunit specifically regulates HIF-1α, but not HIF-1β expression in vivo.

AKT activation was inhibited by siRNA against p110α

The serine–threonine kinase AKT is a well-known target of PI3K. AKT mediates multiple PI3K-induced functions in response to growth factors in vitro. To test whether AKT activity is altered by siP2, we measured the phospho-AKT level in response to PI3K activation in siP2-expressing cells. AKT activation was induced by insulin in the control cells, and was greatly inhibited in siP2-expressing cells, indicating that activation of AKT was affected by siP2. The total AKT level and ERK activation were not affected (Fig. 4A). To determine whether AKT activation is altered by p110α knockdown in vivo, the level of phospho-AKT was determined by immunoblotting using protein extracts from tumor tissue. Similar to the results above, the levels of phospho-AKT were inhibited in tumor tissues expressing siP2 (Fig. 4B). Total AKT and β-actin levels were not affected. These data suggest that siP2 inhibits AKT activation in both ovarian cancer cells and tumors.

SiRNA against AKT1 inhibited angiogenesis and tumor growth

There are three common isoforms of AKT: AKT1/PKBα, AKT2/PKBß, and AKT3/PKB. All three isoforms share a high sequence homology encoded by three separate genes. Accumulating data suggest that roles of AKT/PKB isoforms vary in different cellular processes. AKT1 is the predominant isoform in most tissues, whereas the highest expression of AKT2 has been observed in the insulin-responsive tissues and in some cancer cells (Masure et al., 1999; Kumar et al., 2001). To determine whether AKT1 is required for ovarian tumor growth and angiogenesis, we used siRNA against AKT1 to specifically inhibit AKT1 in ovarian cancer cells. Compared to the scramble siRNA, expression of siA1 and siA2 in the cells suppressed AKT1 mRNA levels, and inhibited insulin-induced AKT

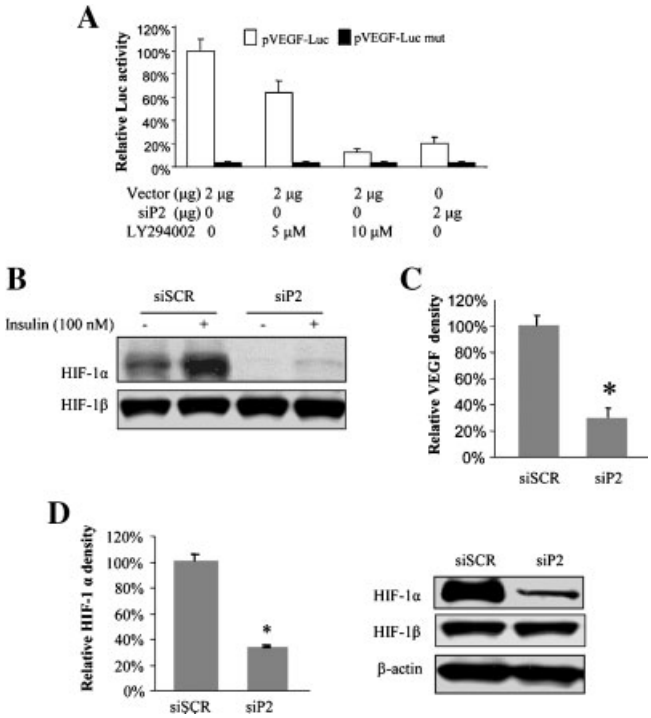

Fig. 3. Inhibition of VEGF transcriptional activation by siP2 is HIF-1α dependent. **A**: To test whether HIF-1 DNA binding is required for siP2-inhibited VEGF transcriptional activation, OVCAR-3 cells were co-transfected with pCMV-β-gal, pMAP11wt and the pSilencer plasmid carrying siP2 or the scramble siRNA. The cells were cultured overnight, then cultured in the absence or presence of 5 μM and 10 μM LY294002 for 12 h to study the luciferase and β-glycosidase activities. OVCAR-3 cells were transfected with pCMV-β-gal, pSilencer-siSCR, pMAP11mut with 3-bp substitution at the HIF-1 DNA binding site in the presence of pSilencer-siP2 construct or LY294002 as indicated. The relative luciferase activity was calculated by the ratio of luc activity/β-gal, and normalized to that of the control. **B**: The serum-starved OVCAR-3 cells expressing siP2 or scramble siRNA were cultured in the absence or presence of 100 nM insulin for 6 h. Aliquots (40 μg) of cellular protein extracts were analyzed by immunoblotting using antibodies specific for HIF-1α and HIF-1β. **C**: The tumor tissue sections were stained with antibodies against VEGF. Relative density of immunofluorescent staining was quantified as described in Materials and Methods. * indicates that the value was significantly different when compared to that of the siSCR ($P < 0.01$). **D**: Left part: The tumor tissue sections were stained with antibodies against HIF-1α. Relative density of immunofluorescent staining was quantified. * indicates that the value was significantly different when compared to that of the siSCR ($P < 0.01$). Right part: Total proteins from tumor lysates were analyzed by immunoblotting with antibodies against HIF-1α, HIF-1β, and β-actin.

phosphorylation (Fig. 4C,D), indicating that AKT1 siRNA was sufficient to inhibit both AKT1 expression and activation. Levels of phospho-ERK1/2, total ERK1/2 and AKT2 protein were not affected (Fig. 4C,D). To test whether AKT1 is required for tumor-induced angiogenesis, we used OVCAR-3 cells stably expressing siA1 or scramble siRNA to assay angiogenesis. The siA1 expression greatly decreased tumor-induced angiogenesis (Fig. 5A,B). SiA1 also decreased tumor growth to 45% of that induced by OVCAR-3 cells expressing scramble siRNA (Fig. 5C). To study whether siA1 decreased tumor cell proliferation, tumor sections were stained using antibodies against PCNA, a mark for evaluating the proliferation. SiA1 greatly decreased PCNA expression in tumor tissues (Fig. 5D), suggesting the inhibition of cell proliferation in tumors. The TUNEL assay was performed to evaluate the effect of siA1 on apoptosis in tumor sections. There was much more apoptosis in tumor tissues expressing siA1 than in those expressing siSCR (Fig. 5E).

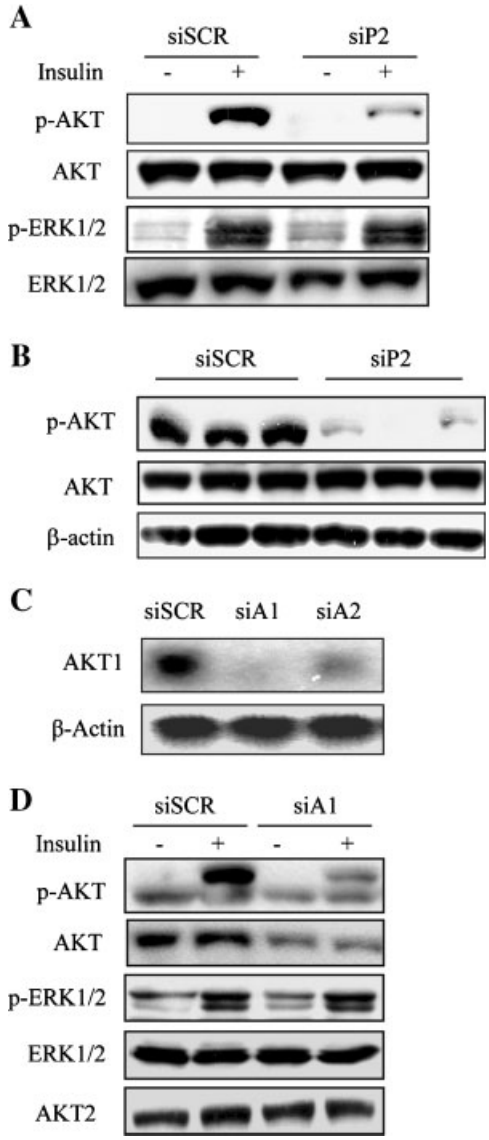

Fig. 4. SiRNAs against PI3K and AKT1 decreased AKT activation. **A**: OVCAR-3 cells expressing siP2 or scramble siRNA were cultured to 90% confluence, followed by serum starvation for 24 h. The cells were then stimulated with 100 nM insulin for 1 h. The total cellular lysates were analyzed by immunoblotting with antibodies against phospho-AKT (ser473), phospho-ERK1/2, total AKT and ERK1/2. Data are representative of at least three independent experiments. **B**: Tumors from the CAM were extracted with lysis buffer and total tumor lysates were analyzed with antibodies against phospho-AKT, total AKT, and β-actin. **C**: siRNA against AKT1 (siA1) decreased AKT expression. OVCAR-3 cells were transfected with the pSilencer vector carrying scramble siRNA or siRNA against AKT1 (siA1 and siA2). After the transfection, cells were selected by 500 μg/ml G418 to obtain stable cell lines. Total RNA expression from the cells was analyzed by Northern blot to detect AKT1 mRNA levels in the cells. β-actin level was used as the control. **D**: SiA1 inhibited insulin-induced AKT activation. OVCAR-3 cells expressing siA1 or the scramble siRNA were cultured to 90% confluence, followed by serum starvation for 24 h. The cells were stimulated with 100 nM insulin for 1 h and harvested. The total cellular lysates were analyzed by immunoblotting with antibodies against phospho-AKT (ser473), phospho-ERK1/2, total AKT, ERK1/2, and AKT2.

SiA1 inhibited VEGF and HIF-1α expression in ovarian cancer cells

To understand whether AKT1 regulates angiogenesis through VEGF expression, we studied the role of AKT1 in the regulation of VEGF and HIF-1α in OVCAR-3 cells. VEGF protein production was measured by ELISA.

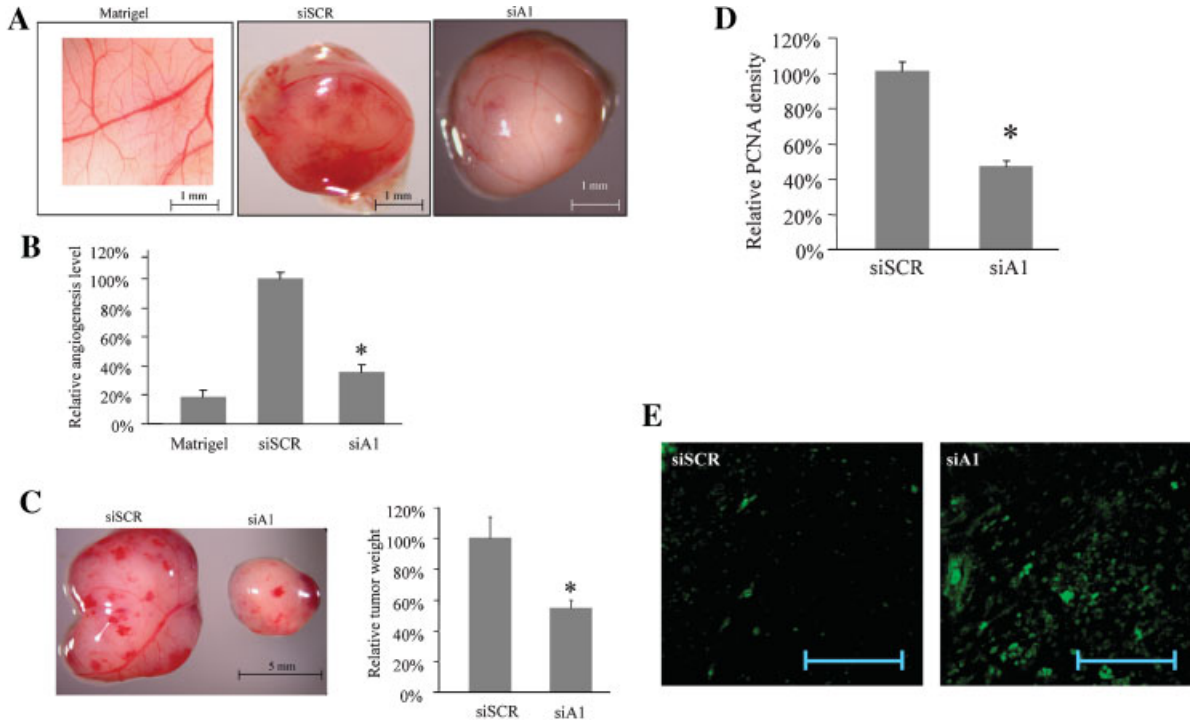

Fig. 5. AKT1 is required for angiogenesis and tumor growth. **A**: 3×10^6 OVCAR-3 cells expressing siA1 or scramble siRNA were mixed with Matrigel, and implanted onto the CAMs of 9-day-old chicken embryos. The Matrigel mixed with medium alone was used as a control. After incubation for 96 h, representative CAM tissues or tumors induced by OVCAR-3 cells were photographed. **B**: The number of blood vessels was obtained by counting the branching of blood vessels, and normalized to the control as relative angiogenesis. The data represent the mean ± SD of the relative angiogenesis from 10 different embryos. * indicates that the value was significantly different when compared to that of the scramble siRNA control ($P < 0.01$). **C**: The cells were implanted onto the CAMs. Tumor growth and the weight were analyzed 9 days after the implantation. Representative tumors are showed (left part). Relative tumor weight was the mean ± SD of tumor weight which was normalized to that of the scramble siRNA control from 10 tumors per treatment (right part). **D**: Tumor sections were stained using antibodies against PCNA. PCNA-positive signals were quantified by digital image analysis, as described in the Materials and Methods. * indicates that the value was significantly different when compared to that of the control ($P < 0.01$). **E**: TUNEL staining. Positively stained fluorescein-labeled tumor sections were visualized and photographed by fluorescence microscopy. The scale bar represents 100 μm.

VEGF production in ovarian cancer cells expressing siA1 was only 40% of the level in the control cells (Fig. 6A). To test how AKT1 regulates VEGF expression in OVCAR-3 cells, we tested the effect of siA1 on VEGF transcriptional activation. The VEGF reporter activity in siA1-expressing cells showed 50% reduction than that in the control cells (Fig. 6B). These data indicated that AKT1 regulated VEGF expression at the transcriptional level. To further investigate the role of siA1 on HIF-1α protein expression, the cells were cultured in serum-free medium overnight, and treated with insulin for 6 h. The cellular lysates were collected and analyzed for HIF-1α expression by immunoblotting. Insulin specifically induced HIF-1α, but not HIF-1β expression in the control cells (Fig. 6C). SiA1 expression abolished HIF-1α expression (Fig. 6C), indicating that AKT1 may activate VEGF transcription specifically through HIF-1α expression in the cells. To determine whether AKT is downstream of PI3K for regulating VEGF transcriptional activation, the cells were cotransfected with siP2 and active form of AKT expression plasmid (myr-Akt). Forced expression of AKT restored siP2-inhibited VEGF reporter activity (Fig. 6D), suggesting that AKT is a sufficient downstream target of PI3K for mediating VEGF transcriptional activation.

SiA1 downregulated VEGF and HIF-1α expression in tumors

The advantage of using siRNA is that we can specifically inhibit AKT1 by stably expressing siA1 in the tumor tissues to study the effect on VEGF and HIF-1 expression. Tumors generated by siA1- and scramble siRNA-expressing cells were sectioned and analyzed using antibodies against HIF-1α. Our results indicated that siA1 inhibited AKT activation, VEGF and HIF-1α expression in the tumors (Fig. 7A–C); however, the inhibitory effects of siA1 were weaker than those of siP2. This could be due to the compensation effects by other AKT isoforms. Western blotting using protein extractions from tumor tissues confirmed that HIF-1α and AKT expression levels were dramatically decreased by siA1 in vivo (Fig. 7D). HIF-1β and β-actin levels were not affected. This indicates that AKT1 specifically affects HIF-1α, but not HIF-1β expression in tumor tissues. These results suggest that AKT1 may regulate ovarian tumor angiogenesis through VEGF and HIF-1α expression in ovarian cancer in vivo.

DISCUSSION

PIK3CA is frequently amplified in ovarian and cervical cancers, and associated with increased p110α protein expression and activity (Wulfkuhle et al., 2003). We recently showed that inhibition of PI3K activity using LY294002 decreased cell proliferation and G_1 progression (Gao et al., 2004). In this study we showed that specific inhibition of p110α subunit in human ovarian cancer cells decreased ovarian tumor growth and angiogenesis in vivo. This result indicated that p110α subunit is a major isoform of PI3K in the regulation of ovarian tumor growth and angiogenesis.

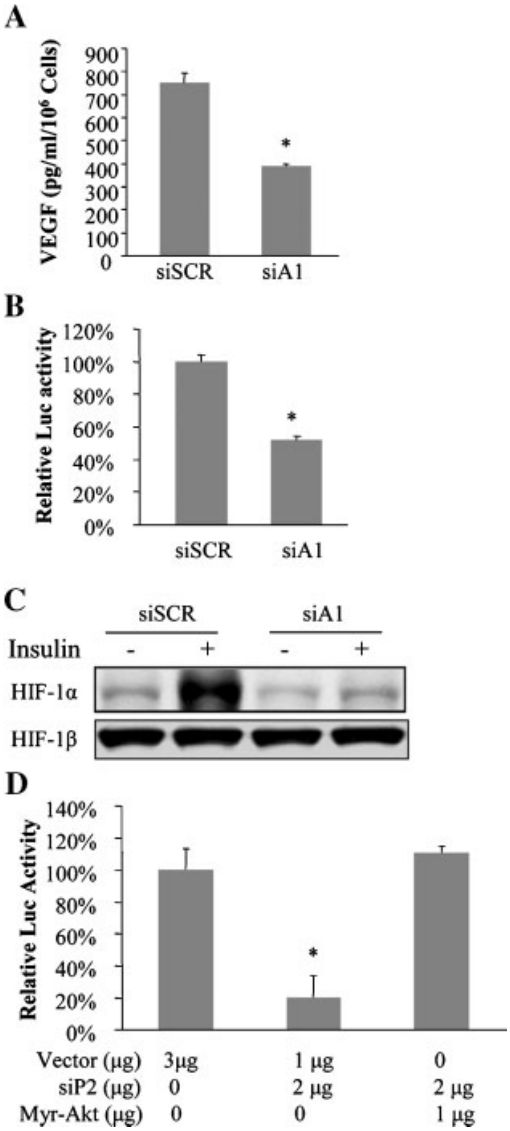

Fig. 6. SiA1 expression decreased VEGF expression via HIF-1α expression. **A**: OVCAR-3 cells expressing siA1 or scramble siRNA were seeded in 12-well plates overnight. The fresh medium was added when the cells reached 90% confluence. The supernatant was collected 24 h after the incubation. VEGF protein levels in the supernatant were determined by ELISA, and divided by the number of cells in each dish. The data are presented as the mean ± SD from three independent experiments with triplicate cultures per experiment. **B**: The cells were seeded at 0.5×10^6 cells/well in 12-well plates, and cultured overnight. The cells were co-transfected with pCMV-β-gal (0.2 μg), pVEGF-Luc (1 μg) and scramble siRNA or siA1 plasmids. The relative luciferase activity was analyzed by the ratio of luc/β-gal activity in the cells 48 h after transfection, and normalized to that of the control. **C:** Serum-starved cells were cultured in the absence or presence of 100 nM insulin for 6 h. Aliquots (40 μg) of cellular protein extracts were analyzed by immunoblotting using antibodies specific for HIF-1α and HIF-1β. **D**: OVCAR-3 cells were co-transfected with pMAP11wt (1 μg), pCMV-β-gal (0.2 μg), pSilencer-siSCR or pSilencer-siP2, and Myr-AKT plasmids as indicated. The relative luc activity was analyzed in the cells as described above.

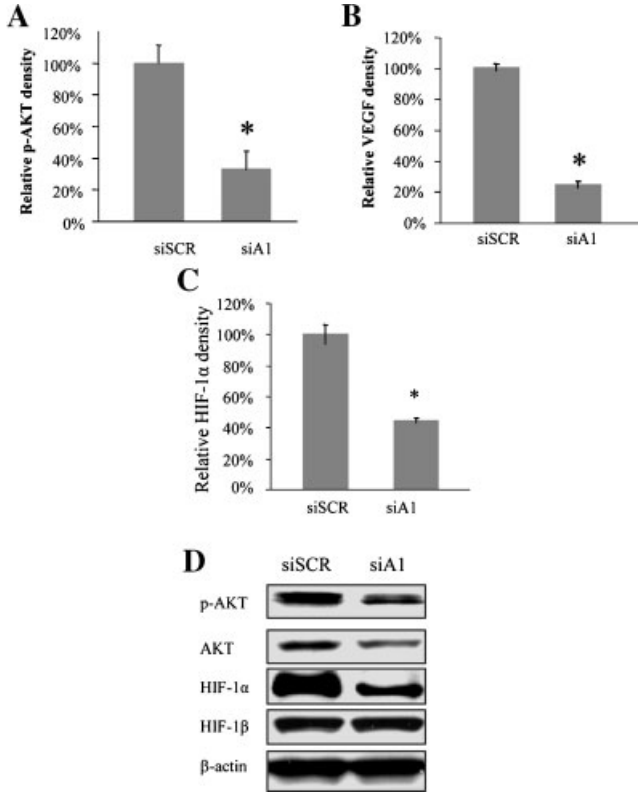

Fig. 7. SiA1 expression inhibited AKT activation, VEGF, HIF-1α, and PCNA expression in tumor tissues. **A**–**C**: Tumor sections from cells expressing scramble siRNA or siA1 were analyzed by immunohistochemistry using antibodies against phospho-AKT (A), VEGF (B), and HIF-1α (C). Immunofluorescent signals were captured with a confocal fluorescence microscope at 40×. Relative signals of immunofluorescent staining were quantified as described in Materials and Methods. * indicates that the value is significantly different when compared to that of the control ($P < 0.01$). **D**: Total tumor tissue lysates were prepared and analyzed by immunoblotting with the antibodies as indicated.

To understand the mechanism of PI3K-mediated angiogenesis, we found that inhibition of p110α subunit decreased VEGF expression via transcriptional activation. It is known that VEGF plays a crucial role in tumor growth and angiogenesis (McMahon, 2000). Oncogenic activation including Ras, Src, and EGFR is known to increase VEGF expression (Goldman et al., 1993; Grugel et al., 1995; Arbiser et al., 1997a; McMahon, 2000). This study showed that specific inhibition of p110α subunit was sufficient to decrease VEGF expression, suggesting that p110α subunit may regulate tumor angiogenesis through VEGF expression. VEGF expression can be regulated either by transcriptional activation or mRNA stability. We used a VEGF promoter reporter gene construct and provided direct evidence that p110α downregulation decreased VEGF expression at the transcriptional level. These data provide an explanation for a previous study that showed the abrogation of ascites by LY294002 treatment, in vivo, in a xenograft i.p. model of ovarian carcinoma because VEGF is directly implicated in ascites formation in ovarian carcinoma (Hu et al., 2000; Hu et al., 2002; Mabuchi et al., 2004). Our data suggest that the targeting of p110α subunit may be useful for the inhibition of tumor angiogenesis. Recent studies showed that VEGF expression is mainly regulated at the transcriptional level through HIF-1 expression (Forsythe et al., 1996a; Maxwell et al., 1997). Our study confirms that p110α subunit regulates VEGF transcriptional activation through HIF-1α, but not HIF-1β subunit expression. We also showed that p110α is required for VEGF and HIF-1α expression in tumor tissues. This study provides strong evidence to suggest that p110α regulate ovarian tumor angiogenesis through VEGF and HIF-1α expression.

AKT is a serine–threonine protein kinase that is activated by PI3K in response to growth factors. Our study demonstrates that AKT activity was substantially decreased by p110α knockdown in vitro and in vivo, indicating that AKT is an important downstream effector of PI3K. To understand which isoform of AKT plays an important role in angiogenesis, we found that AKT1 silencing dramatically inhibited tumor growth and angiogenesis in vivo. We also demonstrated that AKT activity is important for VEGF expression in ovarian cancer cells. To further determine the specific effect of AKT1 inhibition, we showed that Myr-AKT1, a constitutive active form of AKT1, completely reversed the inhibitory effects of siP2-inhibited VEGF reporter activity, indicating that AKT1 is the major isoform for transmitting PI3K-regulated VEGF expression (Fig. 6D). Further evidence from tumor tissue study also supported this finding. Although our data suggested that AKT1 is crucial for tumor growth and angiogenesis in ovarian cancer, it would still be possible that the growth of ovarian cancer cells could escape the control of AKT1 by AKT2 and AKT3 since the three AKTs are differentially regulated in different cell types (Liu et al., 1998; Zinda et al., 2001). The question remains to be investigated. These data implied that AKT1 is the major downstream effector of PI3K in mediating ovarian tumorigenesis and angiogenesis. An interesting result that warrants further investigation is that we demonstrated that the decrease of VEGF expression in ovarian tumor cells correlates with the decrease of PCNA expression. These data suggest that VEGF may not only mediate ovarian tumor angiogenesis, but also stimulate the proliferation of ovarian tumor cells via its receptors. It is possible that the constitutive activation of PI3K pathway through mutations in ovarian cancer cells can directly upregulate the expression of VEGF and HIF-1α, which regulate angiogenesis and cell proliferation. Taken together, our data show that specific inhibition of p110α or AKT1 inhibited ovarian tumor growth and angiogenesis, and inhibited VEGF and HIF-1α expression. These results provide evidence and a mechanism for potentially targeting PI3K and AKT isoforms for human cancer therapy in the future.

LITERATURE CITED

Andrew S. 1999. PIK3CA: Determining its role in cellular proliferation and ovarian cancer. Clin Genet 56:190–191.

Arbiser JL, Moses MA, Fernandez CA, Ghiso N, Cao Y, Klauber N, Frank D, Brownlee M, Flynn E, Parangi S, Byers HR, Folkman J. 1997b. Oncogenic H-ras stimulates tumor angiogenesis by two distinct pathways. Proc Natl Acad Sci USA 94:861–866.

Arsham AM, Plas DR, Thompson CB, Simon MC. 2002. Phosphatidylinositol 3-kinase/Akt signaling is neither required for hypoxic stabilization of HIF-1 alpha nor sufficient for HIF-1-dependent target gene transcription. J Biol Chem 277:15162–15170.

Bedogni B, O'Neill MS, Welford SM, Bouley DM, Giaccia AJ, Denko NC, Powell MB. 2004. Topical treatment with inhibitors of the phosphatidylinositol 3′-kinase/Akt and Raf/mitogen-activated protein kinase kinase/extracellular signal-regulated kinase pathways reduces melanoma development in severe combined immunodeficient mice. Cancer Res 64:2552–2560.

Bertone-Johnson ER. 2005. Epidemiology of ovarian cancer: A status report. Lancet 365:101–102.

Bos JL. 1995. A target for phosphoinositide 3-kinase: Akt/PKB. Trends Biochem Sci 20:441–442.

Broderick DK, Di C, Parrett TJ, Samuels YR, Cummins JM, McLendon RE, Fults DW, Velculescu VE, Bigner DD, Yan H. 2004. Mutations of PIK3CA in anaplastic oligodendrogliomas, high-grade astrocytomas, and medulloblastomas. Cancer Res 64:5048–5050.

Brown LF, Guidi AJ, Schnitt SJ, Van De WL, Iruela-Arispe ML, Yeo TK, Tognazzi K, Dvorak HF. 1999. Vascular stroma formation in carcinoma in situ, invasive carcinoma, and metastatic carcinoma of the breast. Clin Cancer Res 5:1041–1056.

Campbell IG, Russell SE, Choong DY, Montgomery KG, Ciavarella ML, Hooi CS, Cristiano BE, Pearson RB, Phillips WA. 2004. Mutation of the PIK3CA gene in ovarian and breast cancer. Cancer Res 64:7678–7681.

Carpenter CL, Cantley LC. 1990. Phosphoinositide kinases. Biochemistry 29: 11147–11156.

Carpenter CL, Cantley LC. 1996. Phosphoinositide kinases. Curr Opin Cell Biol 8:153–158.

Carpenter CL, Duckworth BC, Auger KR, Cohen B, Schaffhausen BS, Cantley LC. 1990. Purification and characterization of phosphoinositide 3-kinase from rat liver. J Biol Chem 265:19704–19711.

Carpenter CL, Auger KR, Chanudhuri M, Yoakim M, Schaffhausen B, Shoelson S, Cantley LC. 1993. Phosphoinositide 3-kinase is activated by phosphopeptides that bind to the SH2 domains of the 85-kDa subunit. J Biol Chem 268:9478–9483.

Chakravarti A, Zhai G, Suzuki Y, Sarkesh S, Black PM, Muzikansky A, Loeffler JS. 2004. The prognostic significance of phosphatidylinositol 3-kinase pathway activation in human gliomas. J Clin Oncol 22:1926–1933.

Datta K, Bellacosa A, Chan TO, Tsichlis PN. 1996. Akt is a direct target of the phosphatidylinositol 3-kinase. Activation by growth factors, v-src and v-Ha-ras, in Sf9 and mammalian cells. J Biol Chem 271:30835–30839.

Dayanir V, Meyer RD, Lashkari K, Rahimi N. 2001. Identification of tyrosine residues in vascular endothelial growth factor receptor-2/FLK-1 involved in activation of phosphatidylinositol 3-kinase and cell proliferation. J Biol Chem 276:17686–17692.

Fang J, Cao Z, Chen YC, Reed E, Jiang BH. 2004. 9-beta-D-arabinofuranosyl-2-fluoroadenine inhibits expression of vascular endothelial growth factor through hypoxia-inducible factor-1 in human ovarian cancer cells. Mol Pharmacol 66:178–186.

Fang J, Xia C, Cao Z, Zheng JZ, Reed E, Jiang BH. 2005. Apigenin inhibits VEGF and HIF-1 expression via PI3K/AKT/p70S6K1 and HDM2/p53 pathways. FASEB J 19:342–353.

Folkman J. 1971. Tumor angiogenesis: Therapeutic implications. N Engl J Med 285:1182–1186.

Folkman J. 1974. Tumor angiogensis: Role in regulation of tumor growth. Symp Soc Dev Biol 30:43–52.

Forsythe JA, Jiang BH, Iyer NV, Agani F, Leung SW, Koos RD, Semenza GL. 1996c. Activation of vascular endothelial growth factor gene transcription by hypoxia-inducible factor 1. Mol Cell Biol 16:4604–4613.

Franke TF, Kaplan DR, Cantley LC, Toker A. 1997. Direct regulation of the Akt proto-oncogene product by phosphatidylinositol-3,4-bisphosphate. Science 275:665–668.

Gao N, Flynn DC, Zhang Z, Zhong XS, Walker V, Liu KJ, Shi X, Jiang BH. 2004. G1 cell cycle progression and the expression of G1 cyclins are regulated by PI3K/AKT/mTOR/p70S6K1 signaling in human ovarian cancer cells. Am J Physiol Cell Physiol 287:C281–C291.

Goldman CK, Kim J, Wong WL, King V, Brock T, Gillespie GY. 1993. Epidermal growth factor stimulates vascular endothelial growth factor production by human malignant glioma cells: A model of glioblastoma multiforme pathophysiology. Mol Biol Cell 4:121–133.

Grugel S, Finkenzeller G, Weindel K, Barleon B, Marme D. 1995. Both v-Ha-Ras and v-Raf stimulate expression of the vascular endothelial growth factor in NIH 3T3 cells. J Biol Chem 270:25915–25919.

Hallmann D, Trumper K, Trusheim H, Ueki K, Kahn CR, Cantley LC, Fruman DA, Horsch D. 2003. Altered signaling and cell cycle regulation in embryonal stem cells with a disruption of the gene for phosphoinositide 3-kinase regulatory subunit p85alpha. J Biol Chem 278:5099–5108.

Hemmings BA. 1997. Akt signaling: Linking membrane events to life and death decisions. Science 275:628–630.

Hu L, Zaloudek C, Mills GB, Gray J, Jaffe RB. 2000. In vivo and in vitro ovarian carcinoma growth inhibition by a phosphatidylinositol 3-kinase inhibitor (LY294002). Clin Cancer Res 6:880–886.

Hu L, Hofmann J, Lu Y, Mills GB, Jaffe RB. 2002. Inhibition of phosphatidylinositol 3′-kinase increases efficacy of paclitaxel in in vitro and in vivo ovarian cancer models. Cancer Res 62:1087–1092.

Idoate MA, Soria E, Lozano MD, Sola JJ, Panizo A, de Alava E, Manrique M, Pardo-Mindan FJ. 2003. PTEN protein expression correlates with PTEN gene molecular changes but not with VEGF expression in astrocytomas. Diagn Mol Pathol 12:160–165.

Jiang BH, Rue E, Wang GL, Roe R, Semenza GL. 1996. Dimerization, DNA binding, and transactivation properties of hypoxia-inducible factor 1. J Biol Chem 271:17771–17778.

Jiang BH, Zheng JZ, Aoki M, Vogt PK. 2000. Phosphatidylinositol 3-kinase signaling mediates angiogenesis and expression of vascular endothelial growth factor in endothelial cells. Proc Natl Acad Sci USA 97:1749–1753.

Jiang BH, Jiang G, Zheng JZ, Lu Z, Hunter T, Vogt PK. 2001. Phosphatidylinositol 3-kinase signaling controls levels of hypoxia-inducible factor 1. Cell Growth Differ 12:363–369.

Jucker M, Sudel K, Horn S, Sickel M, Wegner W, Fiedler W, Feldman RA. 2002. Expression of a mutated form of the p85alpha regulatory subunit of phosphatidylinositol 3-kinase in a Hodgkin's lymphoma-derived cell line (CO). Leukemia 16:894–901.

Klippel A, Reinhard C, Kavanaugh WM, Apell G, Escobedo MA, Williams LT. 1996. Membrane localization of phosphatidylinositol 3-kinase is sufficient to activate multiple signal-transducing kinase pathways. Mol Cell Biol 16:4117–4127.

Kumar CC, Diao R, Yin Z, Liu Y, Samatar AA, Madison V, Xiao L. 2001. Expression, purification, characterization and homology modeling of active Akt/PKB, a key enzyme involved in cell survival signaling. Biochim Biophys Acta 1526:257–268.

Laughner E, Taghavi P, Chiles K, Mahon PC, Semenza GL. 2001. HER2 (neu) signaling increases the rate of hypoxia-inducible factor 1alpha (HIF-1alpha) synthesis: novel mechanism for HIF-1-mediated vascular endothelial growth factor expression. Mol Cell Biol 21:3995–4004.

Lee JW, Soung YH, Kim SY, Lee HW, Park WS, Nam SW, Kim SH, Lee JY, Yoo NJ, Lee SH. 2005. PIK3CA gene is frequently mutated in breast carcinomas and hepatocellular carcinomas. Oncogene 24:1477–1480.

Liu AX, Testa JR, Hamilton TC, Jove R, Nicosia SV, Cheng JQ. 1998. AKT2, a member of the protein kinase B family, is activated by growth factors, v-Ha-ras, and v-src through phosphatidylinositol 3-kinase in human ovarian epithelial cancer cells. Cancer Res 58:2973–2977.

Ma YY, Wei SJ, Lin YC, Lung JC, Chang TC, Whang-Peng J, Liu JM, Yang DM, Yang WK, Shen CY. 2000. PIK3CA as an oncogene in cervical cancer. Oncogene 19:2739–2744.

Mabuchi S, Ohmichi M, Nishio Y, Hayasaka T, Kimura A, Ohta T, Kawagoe J, Takahashi K, Yada-Hashimoto N, Seino-Noda H, Sakata M, Motoyama T, Kurachi H, Testa JR, Tasaka K, Murata Y. 2004. Inhibition of inhibitor of nuclear factor-kappaB phosphorylation increases the efficacy of paclitaxel in in vitro and in vivo ovarian cancer models. Clin Cancer Res 10:7645–7654.

Marley SB, Lewis JL, Schneider H, Rudd CE, Gordon MY. 2004. Phosphatidylinositol-3 kinase inhibitors reproduce the selective antiproliferative effects of imatinib on chronic myeloid leukaemia progenitor cells. Br J Haematol 125:500–511.

Masure S, Haefner B, Wesselink JJ, Hoefnagel E, Mortier E, Verhasselt P, Tuytelaars A, Gordon R, Richardson A. 1999. Molecular cloning, expression and characterization of the human serine/threonine kinase Akt-3. Eur J Biochem 265:353–360.

Maxwell PH, Dachs GU, Gleadle JM, Nicholls LG, Harris AL, Stratford IJ, Hankinson O, Pugh CW, Ratcliffe PJ. 1997. Hypoxia-inducible factor-1 modulates gene expression in solid tumors and influences both angiogenesis and tumor growth. Proc Natl Acad Sci USA 94:8104–8109.

Mazure NM, Chen EY, Laderoute KR, Giaccia AJ. 1997. Induction of vascular endothelial growth factor by hypoxia is modulated by a phosphatidylinositol 3-kinase/Akt signaling pathway in Ha-ras-transformed cells through a hypoxia inducible factor-1 transcriptional element. Blood 90:3322–3331.

McMahon G. 2000. VEGF receptor signaling in tumor angiogenesis. Oncologist 5(Suppl 1):3–10.

Neufeld G, Cohen T, Gengrinovitch S, Poltorak Z. 1999. Vascular endothelial growth factor (VEGF) and its receptors. FASEB J 13:9–22.

Obata K, Morland SJ, Watson RH, Hitchcock A, Chenevix-Trench G, Thomas EJ, Campbell IG. 1998. Frequent PTEN/MMAC mutations in endometrioid but not serous or mucinous epithelial ovarian tumors. Cancer Res 58:2095–2097.

Philp AJ, Campbell IG, Leet C, Vincan E, Rockman SP, Whitehead RH, Thomas RJ, Phillips WA. 2001. The phosphatidylinositol 3′-kinase p85alpha gene is an oncogene in human ovarian and colon tumors. Cancer Res 61:7426–7429.

Qi JH, Matsumoto T, Huang K, Olausson K, Christofferson R, Claesson-Welsh L. 1999. Phosphoinositide 3 kinase is critical for survival, mitogenesis and migration but not for differentiation of endothelial cells. Angiogenesis 3:371–380.

Rameh LE, Chen CS, Cantley LC. 1995. Phosphatidylinositol (3,4,5)P3 interacts with SH2 domains and modulates PI 3-kinase association with tyrosine-phosphorylated proteins. Cell 83:821–830.

Samuels Y, Velculescu VE. 2004. Oncogenic mutations of PIK3CA in human cancers. Cell Cycle 3:1221–1224.

Samuels Y, Wang Z, Bardelli A, Silliman N, Ptak J, Szabo S, Yan H, Gazdar A, Powell SM, Riggins GJ, Willson JK, Markowitz S, Kinzler KW, Vogelstein B, Velculescu VE. 2004. High frequency of mutations of the PIK3CA gene in human cancers. Science 304:554.

Sansal I, Sellers WR. 2004. The biology and clinical relevance of the PTEN tumor suppressor pathway. J Clin Oncol 22:2954–2963.

Schondorf T, Dostal A, Grabmann J, Gohring UJ. 2000. Single mutations of the PTEN gene in recurrent ovarian carcinomas. J Soc Gynecol Investig 7:313–316.

Semenza GL, Roth PH, Fang HM, Wang GL. 1994. Transcriptional regulation of genes encoding glycolytic enzymes by hypoxia-inducible factor 1. J Biol Chem 269:23757–23763.

Skinner HD, Zheng JZ, Fang J, Agani F, Jiang BH. 2004a. Vascular endothelial growth factor transcriptional activation is mediated by hypoxia-inducible factor 1alpha, HDM2, and p70S6K1 in response to phosphatidylinositol 3-kinase/AKT signaling. J Biol Chem 279:45643–45651.

Skinner HD, Zheng JZ, Fang J, Agani F, Jiang BH. 2004b. Vascular endothelial growth factor transcriptional activation is mediated by hypoxia-inducible factor 1alpha, HDM2, and p70S6K1 in response to phosphatidylinositol 3-kinase/AKT signaling. J Biol Chem 279:45643–45651.

Stein RC. 2001. Prospects for phosphoinositide 3-kinase inhibition as a cancer treatment. Endocr Relat Cancer 8:237–248.

Suzuma K, Naruse K, Suzuma I, Takahara N, Ueki K, Aiello LP, King GL. 2000. Vascular endothelial growth factor induces expression of connective tissue growth factor via KDR, Flt1, and phosphatidylinositol 3-kinase-akt-dependent pathways in retinal vascular cells. J Biol Chem 275:40725–40731.

Thakker GD, Hajjar DP, Muller WA, Rosengart TK. 1999. The role of phosphatidylinositol 3-kinase in vascular endothelial growth factor signaling. J Biol Chem 274:10002–10007.

Tong CY, Hui AB, Yin XL, Pang JC, Zhu XL, Poon WS, Ng HK. 2004. Detection of oncogene amplifications in medulloblastomas by comparative genomic hybridization and array-based comparative genomic hybridization. J Neurosurg Spine 100:187–193.

Trimbos JB, Timmers P. 2004. Chemotherapy for early ovarian cancer. Curr Opin Obstet Gynecol 16:43–48.

Trisciuoglio D, Iervolino A, Zupi G, Del Bufalo D. 2005. Involvement of PI3K and MAPK signaling in bcl-2-induced vascular endothelial growth factor expression in melanoma cells. Mol Biol Cell 16:4153–4162.

Vergote I, Trimbos BJ. 2003. Treatment of patients with early epithelial ovarian cancer. Curr Opin Oncol 15:452–455.

Wang GL, Semenza GL. 1993. Characterization of hypoxia-inducible factor 1 and regulation of DNA binding activity by hypoxia. J Biol Chem 268:21513–21518.

Wulfkuhle JD, Aquino JA, Calvert VS, Fishman DA, Coukos G, Liotta LA, Petricoin EF III, Yokomizo A, Tindall DJ, Hartmann L, Jenkins RB, Smith DI, Liu W. 2003. Signal pathway profiling of ovarian cancer from human tissue specimens using reverse-phase protein microarrays. Proteomics 3:2085–2090.

Yokomizo A, Tindall DJ, Hartmann L, Jenkins RB, Smith DI, Liu W. 1998. Mutation analysis of the putative tumor suppressor PTEN/MMAC1 in human ovarian cancer. Int J Oncol 13:101–105.

Zhong H, Chiles K, Feldser D, Laughner E, Hanrahan C, Georgescu MM, Simons JW, Semenza GL. 2000. Modulation of hypoxia-inducible factor 1alpha expression by the epidermal growth factor/phosphatidylinositol 3-kinase/PTEN/AKT/FRAP pathway in human prostate cancer cells: Implications for tumor angiogenesis and therapeutics. Cancer Res 60:1541–1545.

Zinda MJ, Johnson MA, Paul JD, Horn C, Konicek BW, Lu ZH, Sandusky G, Thomas JE, Neubauer BL, Lai MT, Graff JR. 2001. AKT-1, -2, and -3 are expressed in both normal and tumor tissues of the lung, breast, prostate, and colon. Clin Cancer Res 7:2475–2479.

Zundel W, Schindler C, Haas-Kogan D, Koong A, Kaper F, Chen E, Gottschalk AR, Ryan HE, Johnson RS, Jefferson AB, Stokoe D, Giaccia AJ. 2000. Loss of PTEN facilitates HIF-1-mediated gene expression. Genes Dev 14:391–396.